# Measurement of the $^{8}$Li half-life

X. Fléchard,[1] E. Liénard,[1] O. Naviliat-Cuncic,[1] D. Rodríguez,[2] M. A. G. Alvarez,[3] G. Ban,[1] B. Carniol,[1] D. Etasse,[1] J. M. Fontbonne,[1] A. M. Lallena,[2] and J. Praena[3]

[1]*LPC-Caen, ENSICAEN, Université de Caen Basse-Normandie, CNRS/IN2P3-ENSI, Caen, France*

[2]*Departamento de Física Atómica, Molecular y Nuclear, Universidad de Granada, 18071-Granada, Spain*

[3]*Centro Nacional de Aceleradores, Universidad de Sevilla, Seville, Spain*

(Received 12 July 2010; published 17 August 2010)

We report a new measurement of the $^{8}$Li half-life using a plastic scintillator and an ultrafast waveform digitizing module. The result, $T_{1/2} = (838.40 \pm 0.36)$ ms, improves by a factor of 2.5 the most precise result obtained so far and is furthermore deduced with negligible corrections due to dead time.

DOI: 10.1103/PhysRevC.82.027309 PACS number(s): 21.10.Tg, 27.20.+n

## I. INTRODUCTION

The beta decay of $^{8}$Li offers an attractive structure for the study of fundamental interactions [1–3] and also plays a significant role in nucleosynthesis calculations [4,5]. In particular, the comparison of the $ft$ values between the $\beta^{-}$ and the $\beta^{+}$ Gamow-Teller transitions in this $A = 8$ isospin triplet serves as a means to search for possible second-class currents in the weak interaction [6]. The $^{8}$Li lifetime is also a key parameter in the reaction sequence $^{7}\mathrm{Li}(n,\gamma)^{8}\mathrm{Li}(n,\alpha)^{11}\mathrm{B}$ for inhomogeneous big-bang nucleosynthesis as well as $r$-process nucleosynthesis calculations [4,5] because $^{8}$Li is the bottleneck for the production of light elements with masses $A \geqslant 12$.

The uncertainties of the two most precise and reliable results of the $^{8}$Li half-life, $840.3 \pm 0.9$ ms [7] and $839.6 \pm 1.06$ ms [8], are dominated by statistics. The result quoted in Ref. [7] was obtained after applying a dead-time correction to the data which was a factor of 6.7 larger than the statistical uncertainty.

We report here a new measurement of the $^{8}$Li half-life that was carried out using a plastic scintillator detector and ultrafast readout electronics based on a waveform digitizing module.

## II. EXPERIMENTAL SETUP

The experiment has been performed at the Centro Nacional de Aceleradores (CNA) in Seville, Spain. The $^{8}$Li nuclei were produced via the $^{7}\mathrm{Li}(d,p)^{8}\mathrm{Li}$ reaction initiated with a 1.98-MeV deuteron beam generated by the tandem Van de Graaff accelerator. The typical beam intensity during the measurement was 40 nA.

The measurement was carried out in pulsed mode consisting of activation and decay periods. A regular measuring sequence was composed of a 3-s activation followed by a 17-s decay measurement. The pulsing was accomplished by deflecting the deuteron beam at the exit of the ion source using a Behlke™ switch. Other specific sequences were applied to control possible background contributions.

The target, where the deuteron beam was stopped, was made of a Ø60-mm-diam and 3-mm-thick natural Li cylinder held between two 2-mm-thick plastic pieces. A Ø10-mm aperture on the piece located upstream defined the beam size on the target. The target holder was mounted on a vacuum flange with a Ø60-mm central hole sealed by a 200-$\mu$m-thick aluminum foil. After leaving the target and before they reach the detector, the beta particles from $^{8}$Li decay had then to cross the 2-mm plastic piece located behind the target and the 200-$\mu$m-thick aluminum foil which sealed the vacuum flange.

The beta particles were detected with a $50 \times 67 \times 67$ mm$^3$ BC400 plastic scintillator located outside vacuum, 367-mm downstream from the target. The scintillator was coupled to a XP2020 photomultiplier tube through a Plexiglass light guide glued to one of the small surfaces of the scintillator. The energy spectrum measured by the plastic scintillator during the decay is shown in Fig. 1. The detector was approximately calibrated at low energies using the Compton edges of $\gamma$ rays from a $^{22}$Na source.

The output signal from the photomultiplier base was directly connected to an ultrafast waveform digitizing module, with no other amplification or discrimination stages in between. The module was designed and built at LPC-Caen. Its structure is based on a mother board–daughter board architecture, with the mother board housing specific mezzanine cards. The mother board is connected by Ethernet Gigabit to the control PC. The daughter board includes an embedded PC running under Linux. The communication between the mother and the daughter boards is performed through the local bus via a simple and fast homemade protocol. The signal from the detector, with an amplitude of a few hundreds of mV, is connected to the input front-end on the daughter board. The digital pulse processing function of the module [charge-to-digital converter (QDC), analog-to-digital converter (ADC), or customized] depends on the program which is loaded onto the field-programmable gate array (FPGA) of the daughter board. For this experiment, the QDC function was used. The input signal is continuously sampled at a 500-MHz rate and each amplitude is coded over 12 bits. The data stream resulting from the conversions is continuously written in a circular memory buffer. The trigger occurs when the signal amplitude is larger than a programmable threshold adjusted with a 250-$\mu$V resolution. The digitized amplitudes contained within a programmable time window after the trigger are then made available for the pulse-shape processing. The duration of this window was set to 60 ns and the dead time of the system thereafter is 8 ns. The charge of a pulse within the time window is then calculated by the FPGA on the daughter board by applying an integration algorithm and the result is eventually

 

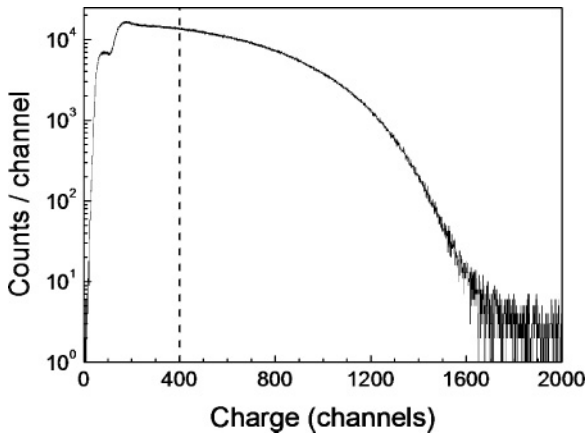


FIG. 1. Charge spectrum of signals from the plastic scintillator associated with the beta particles from $^{8}$Li decay. The vertical dashed line indicates the lower threshold used in the data analysis.

coded over 32 bits. Although the time stamp of the trigger can be defined within 2 ns, such a resolution is not needed for the purpose of the present measurement. The 500-MHz pulses were instead counted in a register resulting in a dwell time of 1.048576 ms per bin in the raw time spectrum. The quartz oscillator used on the daughter board has a frequency stability of 50 ppm. The clock reset on the mother board was synchronized with the signal driving the beam at the ion source in order to obtain the decay curve. In summary, each stored event consists of the coded charge and the corresponding time stamp relative to the external reset. The data were written on the internal hard disk of the control PC.

Figure 2 shows the counting rate for events with a charge above the value indicated by the dashed line in Fig. 1. In order to obtain meaningful fits, the contents of 100 adjacent raw data channels were grouped in a single channel, what eliminates channels without counts. The activation and decay periods are clearly seen. Notice that the decay curve spans a time window of about 12 half-lives before reaching the background rate level. When no software cuts are applied to the data, the maximum measured counting rate at the beginning of the decay period was typically $1.6 \times 10^4$ s$^{-1}$. Since the threshold on the signal was set just above the thermal noise of the photomultiplier, this is also the actual total rate detected by the plastic scintillator. The data were collected over 11 runs having comparable statistics.

## III. DATA ANALYSIS

The model function adopted to fit the decay spectrum contains a single exponential and a constant background

$$f(t) = a \exp(-t/\tau) + b, \tag{1}$$

where $a$, $b$, and $\tau$ are the free parameters and $T_{1/2} = \tau \ln 2$.

The data have first been sorted by defining nine independent windows along the charge spectrum (Fig. 1) in order to obtain sets with comparable statistics. The time spectra were then fitted to study the dependence of the result as a function of the charge. Alternatively, a single decay spectrum was also

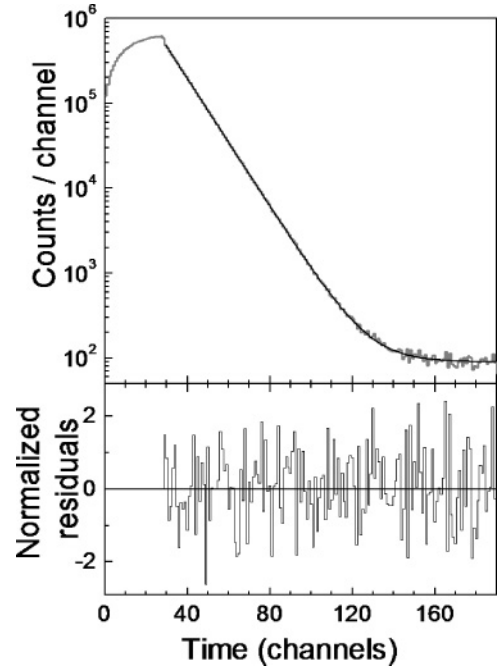


FIG. 2. Upper panel: Histogram of rates measured by the plastic scintillator obtained when applying the threshold indicated by the dashed line in Fig. 1. The time per channel is 104.8576 ms. The black line shows the fit through the data. Lower panel: Normalized residuals over the fitted range.

built and the sensitivity of the result from the fit was studied as a function of the threshold on the charge spectrum. From these tests it was concluded that a threshold corresponding to an energy of about 3 MeV was conservatively safe, leaving sufficient data for the analysis. This threshold is indicated by the dotted line in Fig. 1.

During the off-line analysis, it has been noticed that the signal-to-background ratio, as given, for instance, by the ratio $a/b$, was a factor of 6 larger at the beginning of the experiment than at the end. This was partly due to problems with the ion source and with the beam transport but can also likely be ascribed to activations in the experimental area. Despite this, the values of the half-life obtained from the different runs are statistically consistent, with no correlation observed between the half-life and the signal-to-background ratio.

The weighted mean value obtained from the results of the 11 runs was also checked to be the same as the value obtained by fitting the sum of all data (Fig. 2), indicating that the data display a purely statistical behavior.

The data have also been split in four independent sets and the decay spectra were fitted by changing the initial channel. No significant effect has been found so that the first channel of the fit was selected just after stopping the activation. The decay spectrum was fitted between channels 29 and 190. The result from the fit leads to $T_{1/2} = 838.57 \pm 0.36$ ms with $\chi^2/\nu = 0.9855$ for 158 degrees of freedom. The lower panel in Fig. 2 shows the normalized residuals of the fit, defined as

$$\chi(t) = \frac{r_{\rm exp}(t) - r_{\rm fit}(t)}{\sigma(t)} \tag{2}$$

where $r_{\rm exp}(t) \pm \sigma(t)$ is the measured rate at the time bin $t$ and $r_{\rm fit}(t)$ is the corresponding fitted value. The residuals distribution has been checked to be consistent with a normal distribution.

Rate-dependent losses at any stage of the data acquisition, starting from the detector up to the hard disk, give rise to potential systematic effects. Pile-up events arising during the opening of the 60-ns-long integration window can, in principle, be digitally processed in order to recognize them by pulse-shape analysis but were here counted as single pulses. It is possible to correct the counts per bin in the decay spectrum using the total measured counts $r_{\rm mes}(t)$ (i.e., the counts measured without the software cuts). If $\Delta T$ is the duration of the dead-time window, the corrected rates are

$$r_{\rm cor}(t) = r_{\rm mes}\,(t)[1 + r_{\rm mes}\,(t)\Delta T]. \tag{3}$$

Considering that the effect of the 8-ns dead time of the system is, to first order, identical to pile-up effects arising during the 60-ns integration window, the total dead-time duration was fixed to $\Delta T = 68$ ns. The signal processing and transfer to the PC can handle up to 105 Mbits·s$^{-1}$ which corresponds to an average input pulse rate of $9.4 \times 10^5$ s$^{-1}$. This is a factor of 60 larger that the maximum rate at the detector during the decay measurement. The slowest step in the acquisition chain is the writing of events to disk. The data losses were continuously controlled by a monitoring and display program. No events were lost under the adopted running conditions.

## IV. RESULT AND DISCUSSION

The fit of the time spectrum between channels 29 and 190, corrected following Eq. (3), with the function in Eq. (1) leads to

$$T_{1/2} = 838.40 \pm 0.36 \text{ ms} \tag{4}$$

with $\chi^2/\nu = 1.0103$. The error is purely statistical. Table I summarizes the contributions to the total uncertainty from the sources discussed above.

A comparison with previous measurements is presented in Fig. 3 where the values are plotted according to their respective statistical weight, $1/\sigma^2$, where $\sigma$ is the statistical uncertainty. In this comparison we have excluded all measurements having uncertainties which are at least a factor of 10 larger than the error of the present work. Their inclusion would have had a negligible effect in the determination of the new world average.

TABLE I. Result from the fit and sources of systematic effects along with their contribution to the uncertainty on the half-life.

| Source | Value (ms) | Error (ms) |
|---|---|---|
| Raw data | 838.57 | 0.36 |
| Pile-up | −0.17 | 0.00 |
| Quartz stability | 0.00 | 0.04 |
| Total | 838.40 | 0.36 |

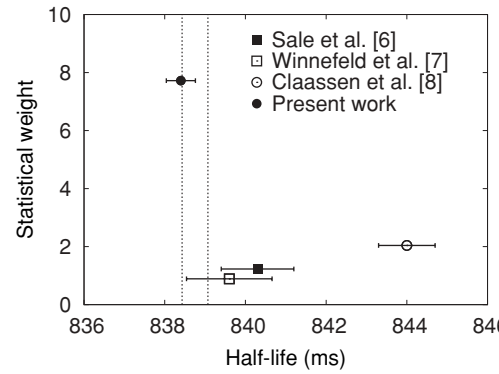


FIG. 3. Experimental values of the $^8$Li half-life having a precision smaller than 3 ms plotted according to their statistical weight. The dotted vertical lines indicate the $\pm 1\sigma$ region of the new world average.

The result from Claassen and Dinter [9] is at variance, at 7.1 combined standard deviations, with the present result. It has already been pointed out [7,8] that the analysis in Ref. [9] did not include any dead-time correction that could partly explain the larger result. One can add to this that the constant background rate level quoted in Ref. [9] does not explain the deviation observed between the data and the single exponential decay for times larger than 7 s. Both effects tend to increase the central value of the half-life.

Excluding the result from Ref. [9] the new world average obtained from the other three values is $(838.75 \pm 0.32)$ ms and is indicated in Fig. 3 by the vertical dotted lines. In contrast to the most precise result from Ref. [7], the value obtained in the present work was extracted with a negligible contribution due to dead time.

## V. CONCLUSION

We have reported a new measurement of the $^8$Li half-life. The result improves by a factor of 2.5 the most precise result obtained so far. Since the dead-time correction applied here is negligible, we consider the present result to be also more reliable.

The data used in the present analysis were collected during a live time of less than 5 h. With available tools and adding a second plastic scintillator it is possible to further improve the statistical precision by an additional factor of 5 in three days of continuous measuring.

## ACKNOWLEDGMENTS

We thank J.A. Labrador and J. García from CNA for their assistance during the experiment. This work has been supported in part by IN2P3-MICINN French-Spanish concerted actions with Contracts Nos. IN2P3-08-14(PN08-1) and FPA2008-04057-E. D.R and A.M.L. acknowledge support also from the Spanish Ministry of Science and Innovation through Project No. FPA2008-04688.

[1] L. Grenacs, Annu. Rev. Nucl. Part. Sci. **35**, 455 (1985).
[2] N. Severijns, M. Beck, and O. Naviliat-Cuncic, Rev. Mod. Phys. **78**, 991 (2006).
[3] T. Sumikama *et al.*, Phys. Lett. B **664**, 235 (2008).
[4] J. H. Applegate, Phys. Rep. **163**, 141 (1988).
[5] G. Wallerstein *et al.*, Rev. Mod. Phys. **69**, 995 (1997).
[6] D. H. Wilkinson and D. E. Alburger, Phys. Rev. Lett. **26**, 1127 (1971).
[7] K. E. Sale *et al.*, Phys. Rev. C **41**, 2418 (1990).
[8] H. Winnefeld *et al.*, Fiz. B **12**, 33 (2003).
[9] D. H. Claassen and H. Dinter, Nucl. Phys. **81**, 155 (1966).